High-Mobility Spin-Polarized Two-Dimensional Electron Gases at $EuO/KTaO_3$ Interfaces

Hongrui Zhang,[1,2,*] Yu Yun,[3,4,*] Xuejing Zhang,[1,2,*] Hui Zhang,[1,2] Yang Ma,[3,4] Xi Yan,[1,2] Fei Wang,[2,5] Gang Li,[1,2] Rui Li,[1,2] Tahira Khan,[1,2] Yuansha Chen,[1,2] Wei Liu,[2,5] Fengxia Hu,[1,2] Banggui Liu,[1,2] Baogen Shen,[1,2] Wei Han,[3,4,†] and Jirong Sun[1,2,‡]

[1]*Beijing National Laboratory for Condensed Matter & Institute of Physics, Chinese Academy of Sciences, Beijing 100190, People's Republic of China*

[2]*University of Chinese Academy of Sciences, Beijing 100049, People's Republic of China*

[3]*International Centre for Quantum Materials, School of Physics, Peking University, Beijing 100871, People's Republic of China*

[4]*Collaborative Innovation Centre of Quantum Matter, Beijing 100871, People's Republic of China*

[5]*Shenyang National Laboratory for Materials Science, Institute of Metal Research, Chinese Academy of Sciences, 72 Wenhua Road, Shenyang 110016, People's Republic of China*

(Received 7 March 2018; revised manuscript received 16 May 2018; published 12 September 2018)

Two-dimensional electron gases (2DEGs) at oxide interfaces, which provide unique playgrounds for emergent phenomena, have attracted increasing attention in recent years. While most of the previous works focused on the 2DEGs at $LaAlO_3/SrTiO_3$ interfaces, here we report on a new kind of 2DEGs formed between a magnetic insulator EuO and a high-k perovskite $KTaO_3$. The 2DEGs are not only highly conducting, with a maximal Hall mobility of 111.6 $cm^2/V\,s$ at 2 K, but also well spin polarized, showing strongly hysteretic magnetoresistance up to 25 K and well-defined anomalous Hall effect up to 70 K. Moreover, unambiguous correspondences between the hysteretic behaviors of 2DEGs and the EuO layer are captured, suggesting the proximity effect of the latter on the former. This is confirmed by the results of density-functional theory calculations: Through interlayer exchange, EuO drives the neighboring TaO_2 layer into a ferromagnetic state. The present work opens new avenues for the exploration for high performance spin-polarized 2DEGs at oxide interfaces.

DOI: 10.1103/PhysRevLett.121.116803

Two-dimensional electron gas (2DEG) at the interfaces between two insulating oxides $LaAlO_3$ (LAO) and $SrTiO_3$ (STO) provides a promising platform for the exploration for emergent phenomena which motivate new concepts for not only fundamental physics but also applied research [1–10]. Unlike the conventional 2DEG formed by s- and p-orbital electrons, the LAO/STO 2DEG is composed of $3d$ electrons. This offers us valuable opportunities to build up magnetic 2DEG, which is centrally important for spintronics. Indeed, x-ray magnetic circular dichroism analysis suggests the appearance of interfacial magnetism [11,12]. Signatures of long range magnetic order were also captured by anomalous Hall effect (AHE) [13–15], magnetoresistance (MR) [16–22], and magnetization [23]. Sometimes magnetic domainlike images were even observed [24–27].

Because of the nonmagnetic nature of LAO and STO, unfortunately, interfacial magnetism is usually weak and appears at very low temperatures. Moreover, magnetic hysteresis, which is a fingerprint of magnetic materials, has been rarely observed for the LAO/STO interfaces [16,17] though negative MR and anisotropic MR have been widely reported [16–22]. The only hysteretic MR appeared at extremely low temperatures (<0.4 K) when Hall mobility is low (several $cm^2/V\,s$ at 2 K) [16]. Although a STO layer sandwiched between two magnetic $GdTiO_3$ layers can be magnetized by magnetic proximity effect [22], magnetism appears only when STO is as thin as 1 nm. Therefore, exploring new ways to get high performance spin-polarized 2DEG remains challenging.

Besides STO-based 2DEGs, there is an important species of electron gases that have been scarcely studied, i.e., the 2DEGs residing in $KTaO_3$ (KTO). In addition to a few examples of 2DEGs generated by electric gating, ionic or UV light irradiation [28–32], the only reported 2DEGs at bilayer interfaces are $LaTiO_3/KTO$ [33] and amorphous-LAO/KTO [34]. Although KTO shares many properties with STO such as high permittivity [31] and quantum paraelectricity [35], it is different from STO as a $5d$ transition metal oxide with strong spin-orbit coupling [29]. Particularly, KTO could be more susceptible to magnetic neighbors since $5d$ electrons are more extended than the $3d$ ones. Here we show that the magnetic proximity effect can be utilized to generate well spin-polarized 2DEGs residing in KTO. Through elaborately controlling the epitaxial growth of the EuO layer on KTO, where EuO acts the same role as the $GdTiO_3$ or $EuTiO_3$ layer in $GdTiO_3/STO/GdTiO_3$ [22]

or LAO/$EuTiO_3$/STO [14], we are successful in achieving high performance 2DEGs that are not only highly conducting but also well spin polarized, exhibiting strongly hysteretic MR up to 25 K and well-defined AHE up to 70 K, while both phenomena were observed before only below, respectively, 0.4 and 10 K for the LAO/STO interfaces [13,14,16,17]. A strong correlation between the magnetic behaviors of the 2DEGs and the EuO film is observed. As revealed by the results of density-functional theory (DFT) calculations, EuO layer drives its neighboring TaO_2 layers into ferromagnetic state, resulting in spin-polarized 2DEGs.

EuO thin films were grown on (001)-oriented KTO single crystal using a molecular beam epitaxy system with a base pressure below 2×10^{-10} mbar [36], see the Supplemental Material (Note 1) for details [37]. Bulk EuO phase crystalizes in a cubic structure with a lattice constant of 5.145 Å. KTO is also cubic with a lattice constant of 3.989 Å. To get an epitaxial growth on KTO, the EuO lattice will rotate along [001] axis by 45° as sketched by Fig. 1(a). In this manner a single crystalline EuO film (9 nm in thickness) was indeed formed as evidenced by the results of reflection high-energy electron diffraction [Fig. 1(b)] and x-ray diffraction (XRD) including the spectra of θ-2θ scan [Fig. 1(c)], ϕ-scan (see Supplemental Material, Fig. S1 [37]), and reciprocal space mapping [Fig. 1(d)]. Fascinatingly, the large lattice mismatch between EuO and KTO (5.15 versus 5.64 Å) does not prevent the epitaxial growth of the EuO film despite of obvious in-plane lattice relaxation [Fig. 1(d)]. The obtained film is very flat with a root mean-squared roughness around 0.36 nm (Supplemental Material, Fig. S2 [37]). According to the XRD spectra, the EuO layer is tetragonal, with an in-plane lattice constant of $a = 5.15$ Å and an out-of-plane lattice parameter of $c = 5.14$ Å.

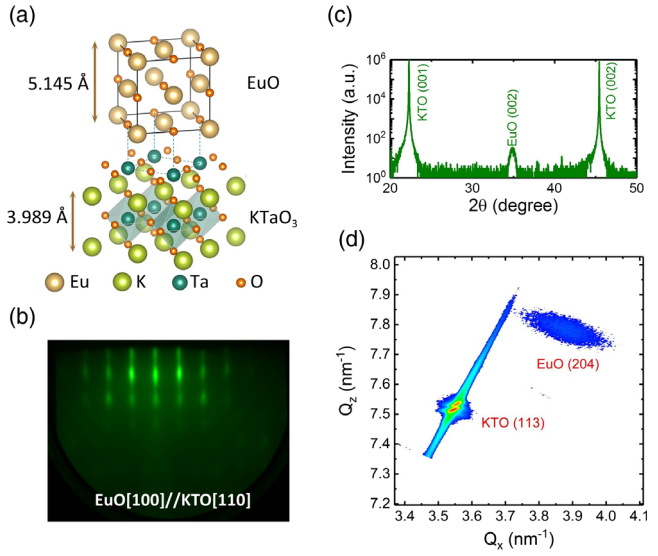

FIG. 1. Crystal structure of the EuO film grown on KTO. (a) A schematic model for the epitaxial growth of EuO on (001) KTO. The EuO lattice has been rotated by 45° around the z axis. (b) Reflection high-energy electron diffraction pattern recorded during the growth process of the EuO layer, clearly showing the EuO[100]//KTO[110] correspondence. (c) θ-2θ x-ray diffraction pattern specifying the well-orientated EuO layer on KTO. (d) Reciprocal space mapping of the (204) reflection of EuO, neighboring the (113) reflection of KTO. The elliptic (204) spot indicates lattice relaxation. All data shown here were obtained for the EuO film grown at a substrate temperature of 450 °C.

EuO thin films obtained here own the standard magnetic properties of the EuO phase. Take the film fabricated at the substrate temperature of $T_S = 450$ °C as an example. The temperature (T) dependent magnetization (M) reordered under an applied field of $H = 0.05$ T indicates that it undergoes a magnetic transition around 71 K [Fig. 2(a)], which is nearly the same as the reported Curie temperature for the EuO phase (70 K), and keeps ferromagnetic down to 5 K, the lowest temperature of the present measurements. The magnetic easy axis lies in the film plane [Fig. 2(b)], and the saturation magnetization is about 6.8 μ_B/Eu, closing to the theoretical value (7 μ_B/Eu^{2+}). M-H loops at higher temperatures were also acquired, which exhibit anticipated reduction in magnetization and coercivity (H_c)

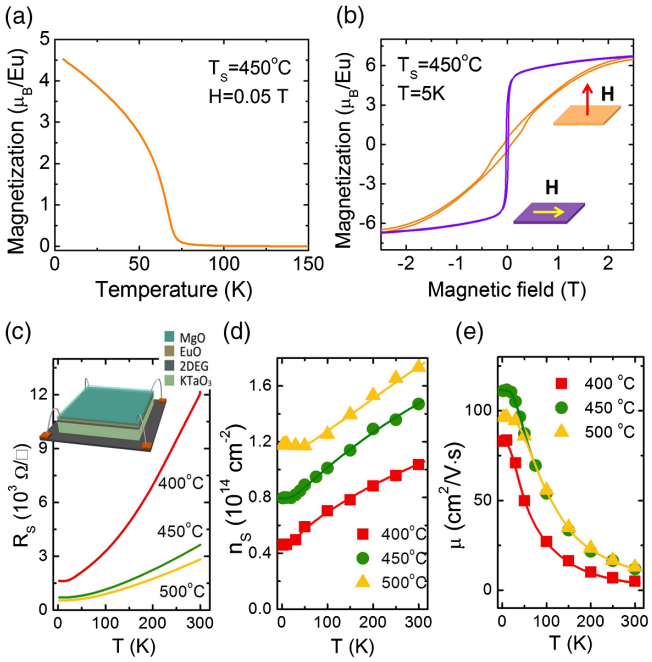

FIG. 2. Magnetic and transport properties of the EuO/KTO heterostructures. (a) Temperature dependence of magnetization of the EuO/KTO heterostructure measured in the field-cooling mode, showing a magnetic onset around 71 K. (b) Magnetic field-dependent magnetizations, measured at 5 K with in-plane and out-of-plane fields, respectively. The easy magnetic axis of the EuO layer lies in film plane. (c) Sheet resistance as a function of temperature. All EuO/KTO interfaces are highly conducting, though detailed resistive behavior varies with fabrication temperature. Inset plot is a sketch for the measurements of sheet resistance and Hall resistance. (d) and (e) Carrier density and Hall mobility, respectively, as functions of temperature.

(Supplemental Material, Fig. S3 [37]). Varying substrate temperature influences slightly the M-T relation but does not the magnetic nature of the EuO film (see Supplemental Material, Fig. S4 [37]).

The EuO/KTO interfaces are well metallic and exhibit the typical feature of two-dimensional conduction, as evidenced by anisotropic magnetoresistance (Supplemental Material, Fig. S5 [37]). A further estimation indicates a conducting layer thickness of ~5.7 nm, which is comparable to the reported thickness for the 2DEG at the LAO/STO interface (2–7 nm) [18,38,39]. Corresponding to T_S of 400, 450, and 500 °C, as shown in Fig. 2(c), the sheet resistance (R_S) is 12.0, 3.6, and 2.8 kΩ/sq at 300 K and 1.6, 0.7, and 0.5 kΩ/sq at 2 K. From 300 to 2 K, R_S experiences approximately a sixfold reduction. As well established, Eu atoms will uptake oxygen from the surface layer of KTO to form EuO phase, generating oxygen vacancies in KTO [36,40,41]. When the content of oxygen vacancies is high enough a metallic 2DEG residing in the interfacial layer of KTO will appear.

Formation of 2DEG at the EuO/KTO interface is further confirmed by Hall effect. The linear Hall resistance at high magnetic field suggests the existence of only one species of charge carrier in the 2DEG. Figure 2(d) presents the deduced carrier density (n_S) of the 2DEG. Corresponding to the fabrication temperature of 400, 450, and 500 °C, the carrier density is 1.0×10^{14}, 1.5×10^{14}, and 1.7×10^{14} cm^{-2} at 300 K and 4.6×10^{13}, 8.0×10^{13}, and 1.2×10^{14} cm^{-2} at 2 K. n_S is in the same order as that of the 2DEG at LAO/STO interface. The carrier density of the present 2DEG displays a monotonic decrease with the decrease of temperature; i.e., the charge carriers are continuously frozen out. This is slightly different from LAO/STO for which charge localization usually appears below 100 K [42,43].

Also, the present 2DEG exhibits considerably high Hall mobility (μ_H). Take the 2DEG obtained at 450 °C as an example. μ_H is 11.8 cm^2/V s at room temperature, slightly larger than that of the STO-based 2DEG, and 111.6 cm^2/V s at 2 K, undergoing a rapid low to high transition upon cooling. This mobility is much higher than that of the only few LAO/STO interfaces showing hysteretic MR (several cm^2/V s) [16], indicating the high performance of the present magnetic 2DEGs.

The most remarkable observation is the hysteretic magnetotransport behaviors. As an example, in Fig. 3(a) we show the MR of the 2DEG prepared at 450 °C, collected at 2 K while cycling magnetic field along the path +0.25 to −0.25 T and to +0.25 T. Two neighboring MR maxima locate at ±0.019 T are observed, forming a butterfly-shaped MR − H curve. This kind of MR effect is the typical feature of metallic magnetic materials, peaking at the coercivity field: Since the structure of magnetic domains is most disordered at H_c, the corresponding resistance is maximal. Therefore, the appearance of hysteretic MR strongly suggests the establishment of magnetic order at the EuO/KTO interface. The maximal MR

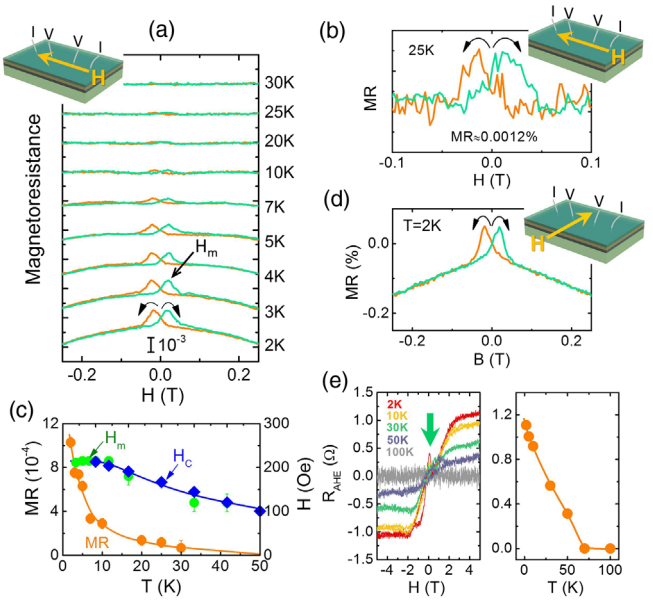

FIG. 3. Magnetotransport properties of the 2DEGs. (a) Magnetoresistance of the 2DEG obtained at 450 °C, measured at different temperatures with the magnetic field parallel to applied current. A constant upward shift was adopted for two successive curves for clarity. Arrows above the curves mark the sweeping direction of the magnetic field. The upper left corner shows the geometry for MR measurements. (b) A magnified view of the MR obtained at 25 K. Upper right corner shows the geometry for MR measurements. (c) Temperature dependence of the maximal MR (origin symbols), the peak position of the MR (green symbols), and the coercive force field of the EuO film (blue symbols). Solid lines are guides for the eye. (d) MR measured at 2 K with the in-plane fields that are perpendicular to the applied current. Upper right corner shows the geometry for MR measurements. (e) Anomalous Hall resistance as a function of magnetic field (left panel) and temperature (right panel) for the 2DEG obtained at 400 °C. Solid line is a guide to the eye. Arrow in the left panel marks the anomaly due to hysteretic MR.

at 2 K is ~0.1%. Increase in temperature causes a rapid decrease in MR. Remarkably, the MR remains identifiable up to 25 K [Fig. 3(b)]. At higher temperatures above 30 K, it is submerged by noises. According to a direct extrapolation, the MR may persist up to 50 K [Fig. 3(c)]. Here we would like to emphasize that the hysteretic MR is a general feature of our 2DEGs, also observed in other samples (see Supplemental Material, Fig. S6 [37]). We also measured the magnetoresistance of the amorphous-LAO/KTO and found no signatures of magnetic hysteresis (Supplemental Material, Fig. S7 [37]). Therefore, the hysteretic MR is a unique feature of the EuO/KTO interface.

To elucidate the mechanism of the resistive hysteresis, we further measured the MR in an in-plane field that is perpendicular to applied current and observed similar MR-H dependences as those in parallel fields [Fig. 3(d)]. Obviously, the MR is not an anisotropic MR that is usually expected for metallic magnetic materials. It stems from an

isotropic depression of magnetic scattering by magnetic field, a typical feature of granular magnetic materials [44].

To confirm the spin polarization of our 2DEGs, AHE is investigated. Figure 3(e) illustrates the anomalous Hall resistance (R_{AHE}) of the 2DEG prepared at 400 °C, obtained by subtracting the linear background from the total R_{xy}-H curve, where R_{xy} is Hall resistance. All R_{AHE}-H curves are step shaped, with the most dramatic changes taking place between −2.5 and 2.5 T. Notably, $H = 2.5$ T is close to the saturation field of the EuO film along perpendicular direction [Fig. 2(b)], as determined from the derivative of magnetization with respect to magnetic field (not shown). It means that the magnetization of the EuO film and the AHE of the 2DEG saturates simultaneously. Remarkably, the R_{AHE} remains sizable up to 50 K; it is 1.1 Ω at 2 K and 0.35 Ω at 50 K. According to a direct extrapolation of the R_{AHE}-T relation, the Curie temperature of the 2DEG is ∼70 K, sevenfold as high as that obtained with a similar procedure for the 2DEG between LAO and STO [13]. The obvious anomalies around $H = 0$ (marked by an arrow) come from hysteretic MR, which cannot be eliminated from the Hall signals.

There are clear indications that the magnetic property of our 2DEG has a close relation to that of EuO. Also shown in Fig. 3(c) is a comparison of the peak position of the MR (H_m, green symbols) and the coercivity field of the EuO film (blue symbols). H_m and H_c match each other very well, indicating a simultaneous reorganization of the magnetic domain structures in EuO and in the interfacial layer of KTO. Under a high enough magnetic field, the magnetic domains are well aligned. As the magnetic field is reduced to the coercivity field, the domain structure becomes most disordered. Thus, its magnetic scattering to charge carriers is the strongest. Moreover, the T_C of the 2DEG is similar to that of the EuO film. A natural explanation is that the magnetic order in the interfacial layer of KTO is induced by neighboring EuO. This inference is supported by the results of DFT calculations as presented below.

Figure 4(a) is the structural model for the DFT calculations following the procedures described in the Supplemental Material (Note 2) [37] and also in Refs. [45–50], i.e., the optimized structure of EuO/KTO superlattices with two oxygen vacancies (O_Vs) in the KTO unit cell adjacent to EuO film (marked by red circles). Figure 4(b) shows the orbital-resolved density of states for the A-site Ta atoms (refer to Supplemental Material Fig. S8 for B-site data and Fig. S9 for Eu atoms at different sites [37]). At the EuO/TaO_2 interface, the two Ta atoms in the first monolayer bond to the two O atoms in the nearest neighbor EuO monolayer with the bond lengths of 1.90 and 2.03 Å, respectively, making the Eu 5d orbit in this EuO monolayer slightly occupied at Fermi energy (see Supplemental Material, Fig. S9 [37]). As a result of the d-f exchange interaction, the Eu 5d states in this EuO layer are spin polarized. This in turn causes a polarization of the Ta

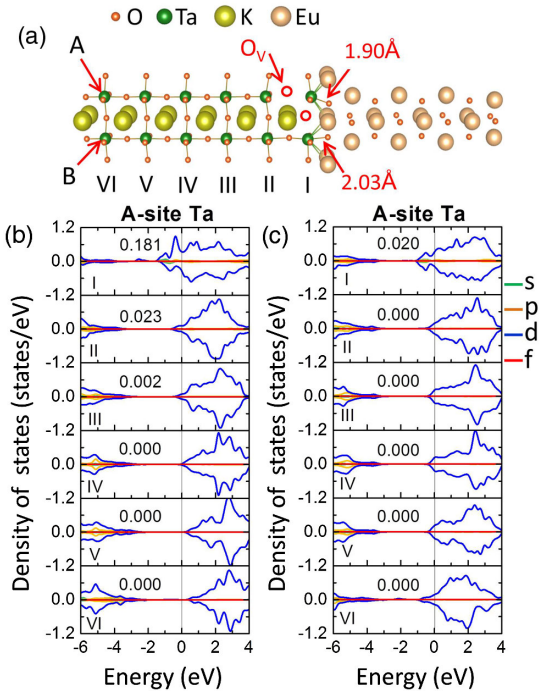

FIG. 4. (a) (EuO_6/KTO_6) superlattices for density-functional theory calculations. (b)-(c) Projected density of states for A-site Ta atoms, obtained for the TaO_2/EuO (b) and KO/EuO (c) interfaces. Positive and negative densities of states represent the spin-up and spin-down states, respectively. Numbers in the figure indicate the net magnetization in the unit of μ_B/Ta.

5d states in the neighboring TaO_2 due to the Eu-5d and Ta-5d hybridization. In Fig. 4(b) we also presented the calculated magnetic moments of each Ta atom. Since the A-site interfacial Ta atom is closer to the neighboring Eu atoms than the B-site one (3.23 and 3.30 Å as compared to 3.38 and 3.52 Å), it has a larger magnetic moment than the B-site one (∼0.181 μ_B versus 0.096 μ_B). According to these results, it is clear that ferromagnetic order can be induced at the EuO/TaO_2 interface by magnetic EuO. We performed similar calculations for the (EuO/KO) interface and, fascinatingly, observed no spin polarization for the Ta 5d states [Fig. 4(c)], though the EuO/KO interface is conducting.

In the model for our DFT calculations, oxygen vacancies in KTO are assumed to exist only in the first unit cell neighboring EuO. A direct calculation based on the band structure in Fig. 4(b) yields the carrier density of $\sim 4.8 \times 10^{14}$ cm^{-2}, while the experimental result is $\sim 1.7 \times 10^{14}$ cm^{-2}. This difference could be attributed to localized charge carriers, similar to the case in LAO/STO interfaces [42,43].

Since it is difficult to obtain a single terminated layer surface for the (001) KTO due to its polar nature, EuO/TaO_2 and EuO/KO interfaces thus magnetic and nonmagnetic domains may coexist at the EuO/KTO interface, resulting in considerable magnetic scattering to itinerant electrons. When the magnetic domains are

orientated by external field, considerably MR will appear due to the depression of spin scattering if the separation between magnetic domains is within the mean free path of charge carriers of the 2DEG. In this case, the MR is independent of the direction of magnetic field with respect to applied current, like that observed in the heterogeneous materials composed of magnetic grains dispersed in metallic matrix [44]. To confirm this inference, we performed an analysis of the surface morphology of KTO (see Supplemental Material, Fig. S10 [37]). By marking the areas with the height difference of a unit cell, which have the same terminated layer, with the same color and the ones with just half a unit cell height difference by a different color, we obtained an image with maze domains, formed by intertwined two kinds of surface layers (blue and cyan areas) delimited by transition regions (yellow areas). Obviously, our 2DEGs could be magnetically inhomogeneous as assumed above, exhibiting an isotropic MR under applied field.

Finally, we would like to give a brief explanation to the discrepancy between the calculated (∼2.4 nm) and experimentally estimated (∼5.7 nm) thickness of 2DEGs. This could be ascribed to the simplified DFT model which assumes the existence of oxygen vacancies only in the first unit cell neighboring EuO to capture the main feature of the proximity effect. In general, oxygen vacancies may also exist in inner unit cells, resulting in thicker 2DEGs.

In summary, spin polarized 2DEGs have been obtained by growing insulating EuO epitaxial films on high-k KTO crystals. The 2DEG thus obtained is not only highly conducting but also well spin polarized, showing obviously hysteretic magnetoresistance against magnetic cycling and well-defined anomalous Hall effect. Remarkably, the Curie temperature deduced from anomalous Hall effect is ∼70 K, which is sevenfold as high as the reported value determined with the similar procedure for the 2DEGs composed of nonmagnetic oxides. A strong correlation between the magnetic behaviors of the 2DEGs and the EuO film is captured. Further analysis shows that the magnetic EuO produces a strong effect on neighboring KTO, driving the TaO_2 interfacial layer into the ferromagnetic state. The present work demonstrates the great potential of magnetic oxide interfaces for new concept materials or devices of spintronics.

This work has been supported by the National Basic Research of China (2016YFA0300701, 2015CB921104, 2017YFA0206300, and 2014CB920902), the National Natural Science Foundation of China (11520101002, 11574006, 51590880, 51531008, and 11704011), and the Key Program of the Chinese Academy of Sciences.

*These authors contributed equally to this work.
†Corresponding author.
weihan@pku.edu.cn
‡Corresponding author.
jrsun@iphy.ac.cn

[1] A. Ohtomo and H. Y. Hwang, Nature (London) **427**, 423 (2004).
[2] A. D. Caviglia, S. Gariglio, N. Reyren, D. Jaccard, T. Schneider, M. Gabay, S. Thiel, G. Hammerl, J. Mannhart, and J. M. Triscone, Nature (London) **456**, 624 (2008).
[3] G. Herranz, G. Singh, N. Bergeal, A. Jouan, J. Lesueur, J. Gázquez, M. Varela, M. Scigaj, N. Dix, F. Sanchez, and J. Fontcuberta, Nat. Commun. **6**, 6028 (2015).
[4] A. D. Caviglia, M. Gabay, S. Gariglio, N. Reyren, C. Cancellieri, and J. M. Triscone, Phys. Rev. Lett. **104**, 126803 (2010).
[5] Q. Song, H. R. Zhang, T. Su, W. Yuan, Y. Y. Chen, W. Y. Xing, J. Shi, J. R. Sun, and W. Han, Sci. Adv. **3**, e1602312 (2017).
[6] E. Lesne, Y. Fu, S. Oyarzun, J. C. Rojas-Sánchez, D. C. Vaz, H. Naganuma, G. Sicoli, J. P. Attane, M. Jamet, E. Jacquet, J. M. George, A. Barthélémy, H. Jaffrès, A. Fert, M. Bibes, and L. Vila, Nat. Mater. **15**, 1261 (2016).
[7] Y. Wang, R. Ramaswamy, M. Motapothula, K. Narayanapillai, D. P. Zhu, J. W. Yu, T. Venkatesan, and H. Yang, Nano Lett. **17**, 7659 (2017).
[8] H. H. Chen, A. M. Kolpak, and S. Ismail-Beigi, Adv. Mater. **22**, 2881 (2010).
[9] P. Delugas, A. Filippetti, V. Fiorentini, D. I. Bilc, D. Fontaine, and P. Ghosez, Phys. Rev. Lett. **106**, 166807 (2011).
[10] G. Singh-Bhalla, C. Bell, J. Ravichandran, and W. SiemonsY. Hikita, S. Salahuddin, A. F. Hebard, H. Y. Hwang, and R. Ramesh, Nat. Phys. **7**, 80 (2011).
[11] J. S. Lee, Y. W. Xie, H. K. Sato, C. Bell, Y. Hikita, H. Y. Hwang, and C. C. Kao, Nat. Mater. **12**, 703 (2013).
[12] M. Salluzzo, S. Gariglio, D. Stornaiuolo, V. Sessi, S. Rusponi, C. Piamonteze, G. M. De Luca, M. Minola, D. Marré, A. Gadaleta, H. Brune, F. Nolting, N. B. Brookes, and G. Ghiringhelli, Phys. Rev. Lett. **111**, 087204 (2013).
[13] F. Gunkel, C. Bell, H. Inoue, B. Kim, A. G. Swartz, T. A. Merz, Y. Hikita, S. Harashima, H. K. Sato, M. Minohara, S. Hoffmann-Eifert, R. Dittmann, and H. Y. Hwang, Phys. Rev. X **6**, 031035 (2016).
[14] D. Stornaiuolo, C. Cantoni, G. M. De Luca, R. Di Capua, E. Di Gennaro, G. Ghiringhelli, B. Jouault, D. Marrè, D. Massarotti, F. Miletto Granozio, I. Pallecchi, C. Piamonteze, S. Rusponi, F. Tafuri, and M. Salluzzo, Nat. Mater. **15**, 278 (2016).
[15] A. Joshua, J. Ruhman, S. Pecker, E. Altman, and S. Ilani, Proc. Natl. Acad. Sci. U.S.A. **110**, 9633 (2013).
[16] A. Brinkman, M. Huijben, M. van Zalk, J. Huijben, U. Zeitler, J. C. Maan, W. G. van der Wiel, G. Rijnders, D. H. A. Blank, and H. Hilgenkamp, Nat. Mater. **6**, 493 (2007).
[17] D. A. Dikin, M. Mehta, C. W. Bark, C. M. Folkman, C. B. Eom, and V. Chandrasekhar, Phys. Rev. Lett. **107**, 056802 (2011).
[18] M. Ben Shalom, C. W. Tai, Y. Lereah, M. Sachs, E. Levy, D. Rakhmilevitch, A. Palevski, and Y. Dagan, Phys. Rev. B **80**, 140403(R) (2009).
[19] J. H. Ngai, Y. Segal, D. Su, Y. Zhu, F. J. Walker, S. Ismail-Beigi, K. Le Hur, and C. H. Ahn, Phys. Rev. B **81**, 241307(R) (2010).

[20] X. Wang, W. M. Lü, A. Annadi, Z. Q. Liu, K. Gopinadhan, S. Dhar, T. Venkatesan, and Ariando, Phys. Rev. B **84**, 075312 (2011).
[21] E. Flekser, M. Ben Shalom, M. Kim, C. Bell, Y. Hikita, H. Y. Hwang, and Y. Dagan, Phys. Rev. B **86**, 121104(R) (2012).
[22] P. Moetakef, J. R. Williams, D. G. Ouellette, A. P. Kajdos, D. Goldhaber-Gordon, S. J. Allen, and S. Stemmer, Phys. Rev. X **2**, 021014 (2012).
[23] Ariando, X. Wang, G. Baskaran, Z. Q. Liu, J. Huijben, J. B. Yi, A. Annadi, A. R. Barman, A. Rusydi, S. Dhar, Y. P. Feng, J. Ding, H. Hilgenkamp, and T. Venkatesan, Nat. Commun. **2**, 188 (2011).
[24] J. A. Bert, B. Kalisky, C. Bell, M. Kim, Y. Hikita, H. Y. Hwang, and K. A. Moler, Nat. Phys. **7**, 767 (2011).
[25] B. Kalisky, J. A. Bert, C. Bell, Y. W. Xie, H. K. Sato, M. Hosoda, Y. Hikita, H. Y. Hwang, and K. A. Moler, Nano Lett. **12**, 4055 (2012).
[26] B. Kalisky, J. A. Bert, B. B. Klopfer, C. Bell, H. K. Sato, M. Hosoda, Y. Hikita, H. Y. Hwang, and K. A. Moler, Nat. Commun. **3**, 922 (2012).
[27] F. Bi, M. C. Huang, S. Ryu, H. Lee, C. W. Bark, C. B. Eom, P. Irvin, and J. Levy, Nat. Commun. **5**, 5019 (2014).
[28] H. Nakamura and T. Kimura, Phys. Rev. B **80**, 121308(R) (2009).
[29] P. D. C. King, R. H. He, T. Eknapakul, P. Buaphet, S.-K. Mo, Y. Kaneko, S. Harashima, Y. Hikita, M. S. Bahramy, C. Bell, Z. Hussain, Y. Tokura, Z.-X. Shen, H. Y. Hwang, F. Baumberger, and W. Meevasana, Phys. Rev. Lett. **108**, 117602 (2012).
[30] A. F. Santander-Syro, C. Bareille, F. Fortuna, O. Copie, M. Gabay, F. Bertran, A. Taleb-Ibrahimi, P. Le Fèvre, G. Herranz, N. Reyren, M. Bibes, A. Barthélémy, P. Lecoeur, J. Guevara, and M. J. Rozenberg, Phys. Rev. B **86**, 121107 (R) (2012).
[31] S. Harashima, C. Bell, M. Kim, T. Yajima, Y. Hikita, and H. Y. Hwang, Phys. Rev. B **88**, 085102 (2013).
[32] C. Bareille, F. Fortuna, T. C. Rödel, F. Bertran, M. Gabay, O. Hijano Cubelos, A. Taleb-Ibrahimi, P. Le Fèvre, M. Bibes, A. Barthélémy, T. Maroutian, P. Lecoeur, M. J. Rozenberg, and A. F. Santander-Syro, Sci. Rep. **4**, 3586 (2014).
[33] K. Zou, S. Ismail-Beigi, K. Kisslinger, X. Shen, D. Su, F. J. Walker, and C. H. Ahn, APL Mater. **3**, 036104 (2015).
[34] H. Zhang, H. R. Zhang, X. Yan, X. J. Zhang, Q. H. Zhang, J. Zhang, F. R. Han, L. Gu, B. G. Liu, Y. S. Chen, B. S. Shen, and J. R. Sun, ACS Appl. Mater. Interfaces **9**, 36456 (2017).
[35] U. T. Höchli, H. E. Weibel, and L. A. Boatner, Phys. Rev. Lett. **39**, 1158 (1977).
[36] R. Sutarto, S. G. Altendorf, B. Coloru, M. Moretti Sala, T. Haupricht, C. F. Chang, Z. Hu, C. Schüßler-Langeheine, N. Hollmann, H. Kierspel, H. H. Hsieh, H. J. Lin, C. T. Chen, and L. H. Tjeng, Phys. Rev. B **79**, 205318 (2009).
[37] See Supplemental Material at http://link.aps.org/supplemental/10.1103/PhysRevLett.121.116803 for experimental details and additional experimental data.
[38] M. Basletic, J.-L. Maurice, C. Carrétéro, G. Herranz, O. Copie, M. Bibes, É. Jacquet, K. Bouzehouane, S. Fusil, and A. Barthélémy, Nat. Mater. **7**, 621 (2008).
[39] O. Copie, V. Garcia, C. Bödefeld, C. Carrétéro, M. Bibes, G. Herranz, E. Jacquet, J.-L. Maurice, B. Vinter, S. Fusil, K. Bouzehouane, H. Jaffrès, and A. Barthélémy, Phys. Rev. Lett. **102**, 216804 (2009).
[40] P. Lömker, T. C. Rödel, T. Gerber, F. Fortuna, E. Frantzeskakis, P. Le Fèvre, F. Bertran, M. Müller, and A. F. Santander-Syro, Phys. Rev. Mater. **1**, 062001(R) (2017).
[41] Y. Yun, Y. Ma, T. Su, W. Y. Xing, Y. Y. Chen, Y. Y. Yao, R. R. Cai, W. Yuan, and W. Han, Phys. Rev. Mater. **2**, 034201 (2018).
[42] Y. Z. Chen, N. Pryds, J. E. Kleibeuker, G. Koster, J. R. Sun, E. Stamate, B. G. Shen, G. Rijnders, and S. Linderoth, Nano Lett. **11**, 3774 (2011).
[43] Z. Q. Liu, C. J. Li, W. M. Lü, X. H. Huang, Z. Huang, S. W. Zeng, X. P. Qiu, L. S. Huang, A. Annadi, J. S. Chen, J. M. D. Coey, and T. Venkatesan, and Ariando, Phys. Rev. X **3**, 021010 (2013).
[44] J. Q. Xiao, J. S. Jiang, and C. L. Chien, Phys. Rev. Lett. **68**, 3749 (1992).
[45] P. Hohenberg and W. Kohn, Phys. Rev. **136**, B864 (1964).
[46] W. Kohn and L. J. Sham, Phys. Rev. **140**, A1133 (1965).
[47] G. Kresse and D. Joubert, Phys. Rev. B **59**, 1758 (1999).
[48] P. E. Blöchl, Phys. Rev. B **50**, 17953 (1994).
[49] J. P. Perdew, K. Burke, and M. Ernzerhof, Phys. Rev. Lett. **77**, 3865 (1996).
[50] J. P. Perdew, A. Ruzsinszky, G. I. Csonka, O. A. Vydrov, G. E. Scuseria, L. A. Constantin, X. Zhou, and K. Burke, Phys. Rev. Lett. **100**, 136406 (2008).